2026 11th IEEE RAS/EMBS International Conference for
Biomedical Robotics and Biomechatronics (BioRob)
August 1-4 2026. Edmonton, Canada

PrintExo: An Open-Source, Shoe-Agnostic, 3D-Printable Ankle Exoskeleton Platform for Accessible Locomotion Research

Sunin Baek[1†], Yuhyeon Lee[1†], Benjamin Hur[1], Eun Sang Cha[1], and Daekyum Kim[1,2*]

Abstract— **Wearable ankle exoskeletons are a key testbed for assistive control and human-robot interaction during locomotion, but many systems remain difficult to build and deploy due to fabrication and fitting overhead (e.g., computer numerical control (CNC) machining or composite processes, long lead times, and shoe-specific interfaces). We present PrintExo, an open-source, shoe-agnostic, fully 3D-printable ankle exoskeleton platform designed to lower the barrier to early-stage locomotion research and rapid prototyping. PrintExo can be fabricated using consumer-grade fused deposition modeling (FDM) 3D printing and standard off-the-shelf components, and integrates a compact 3D-printed 1:4 planetary gearbox for ankle assistance (total assembled mass: 1.33 kg per leg, excluding the user's shoe). A lace-anchored shoe interface transmits torque through commercially available lace-up footwear without permanent modification, enabling fast fitting across participants. The device was evaluated in a feasibility pilot treadmill study with five able-bodied participants walking at 1.0 m/s under three conditions: no-device, zero-torque, and powered assistance, and was reused sequentially across participants. Across completed sessions, gross metabolic power was lower under powered assistance than under zero-torque, and encoder-derived kinematics captured device-side ankle motion during torque application. Overall, PrintExo provides a practical, low-overhead, open-source platform for accessible ankle-exoskeleton prototyping and pilot locomotion experiments.**

I. INTRODUCTION

Interest in wearable lower-limb exoskeletons is growing for applications in gait assistance [1], [2], rehabilitation [3], [4], and performance augmentation [5], [6]. These systems typically provide assistive torque based on estimates of gait phase and gait kinematics to improve locomotor performance and reduce metabolic cost [7]. Among various joints, the ankle is a key joint of interest for research because it contributes significantly to propulsion during the push-off phase of walking [8]. Ankle-assistive devices are well-studied with reported metabolic benefits, and their relatively simple degree of freedom makes them an ideal testbed for evaluating new control strategies or biomechanical responses [9]. However, despite the scientific significance of ankle-assistive devices, initiating research in this area still requires overcoming substantial practical barriers before experimental studies can even begin [10].

In practice, establishing a research infrastructure for ankle exoskeletons involves significant interdisciplinary challenges, including actuation, wearable sensors, mechanical design, and control strategy [11]. Unlike many non-wearable robotics domains (e.g., robotic arms [12], [13], aerial robots [14], or mobile robots [15]) where benchtop or low-fidelity prototypes can serve as entry-level tools, wearable systems require attachment to the human body and load-bearing integrity from the outset [16], [17]. As a result, experimental ankle exoskeleton hardware must withstand dynamic gait forces and maintain consistent alignment with the biological joint to be viable for locomotion experiments with human participants [18], [19]. Furthermore, traditional manufacturing methods such as computer numerical control (CNC) machining or carbon fiber molding require expensive infrastructure and involve long fabrication lead times [20]. Practical challenges also arise during the setup and fitting process, where repeated customization for different footwear and user-specific body dimensions requires substantial time and resources [21], [22]. While a notable open-source initiative has begun to address these issues [10], a platform that is easy to fabricate and fit while remaining reproducible is still lacking.

To address these barriers, we present PrintExo, an open-source, shoe-agnostic, 3D-printable ankle exoskeleton platform that minimizes fabrication and fitting overhead for early-stage locomotion research with human participants. The system utilizes consumer-grade fused deposition modeling (FDM) 3D printing and standard off-the-shelf components to simplify the manufacturing process. The actuation module integrates a 3D-printed 1:4 planetary gear stage, enabling ankle-assistance experiments in a fully printable, compact form factor. Furthermore, PrintExo incorporates a lace-anchored shoe interface that attaches securely across a wide range of lace-up footwear without permanent modification. To demonstrate functional feasibility, we conducted a pilot treadmill study with five participants to evaluate structural durability, gross metabolic power, and encoder-derived ankle kinematics.

PrintExo is released as an open-source platform, including editable computer-aided design (CAD) files, print-ready manufacturing assets, assembly manuals, and a complete bill of materials, to support reproducibility and implementation (`https://printexo.github.io`). Together, the open-source release and pilot feasibility results support the use of PrintExo as a practical testbed for early-stage ankle-assistance research and educational settings.

This work was supported by the Korean ARPA-H Project through KHIDI (MOHW), Republic of Korea (RS-2025-25455839).

[1]School of Mechanical Engineering, Korea University, Seoul, South Korea

[2]School of Smart Mobility, Korea University, Seoul, South Korea

†These authors contributed equally to this work

*Corresponding author: Daekyum Kim, Ph.D.

II. Related work

Most lower-limb exoskeletons remain closed-source, limiting replication and customization for research use. To support reproducibility, several studies have released CAD files and control software as supplementary materials [2], [23]–[25]. However, these hardware designs often require specialized fabrication that remains inaccessible for many researchers. For instance, existing designs frequently require high-strength carbon fiber components [2], [23], custom aluminum sheet-metal assemblies [24], or hybrid structures utilizing both materials that require industrial waterjet-cutting or CNC machining [25]. Even modular platforms such as OpenExo, which aim to improve accessibility, can still require custom-ordered parts and professional machining [10]. This suggests that manufacturing accessibility remains an open challenge in wearable robotics, motivating the need for a more accessible platform that enables rapid, independent replication without extensive manufacturing infrastructure.

Additive manufacturing offers a practical path to bypass complex fabrication, providing high accessibility through rapid prototyping. The efficacy of this approach has been well-demonstrated in the upper-limb domain, including the development of fully 3D-printed hand exoskeletons for rehabilitation [26], [27], rapid prototyping toolkits for arm-based exoskeletons [28], and functional passive upper-limb exoskeletons [29]. Despite these advancements, the application of 3D printing to lower-limb systems remains notably underexplored within the open-source community. This research gap originates from the intense mechanical demands of human locomotion, where adult-sized devices must sustain substantial loads and repetitive impacts that have traditionally required high-strength materials like metal [30]. Consequently, the challenge of balancing manufacturing simplicity with the structural demands of locomotion remains a key bottleneck, limiting the availability of reliable, accessible 3D-printed lower-limb platforms. Addressing this bottleneck requires load-aware mechanical design and a clearly defined operating scope, rather than attempting to match the durability of high-duty exoskeleton systems.

Beyond the challenges of structural fabrication, the interface between the exoskeleton and the user's footwear presents another critical barrier to accessibility. To achieve the mechanically stiff anchoring required for effective torque transmission, many existing systems rely on attachment methods that require permanent modifications to the shoe, such as drilling through the outsole to secure carbon-fiber or metal footplates [2], [31]. Alternatively, some designs utilize internal interfaces that are positioned in direct contact with the user's foot inside the shoe [24], [32], [33]. However, these approaches often necessitate custom-machined metal components tailored to individual foot geometries, which increases fabrication complexity and limits the range of compatible footwear. PrintExo addresses this gap with a fully 3D-printable, lace-anchored shoe interface that enables shoe-agnostic, stiff anchoring for torque transfer without drilling the outsole or relying on personalized metal components.

III. System Design

A. Design Objectives

The primary design objective of PrintExo is to lower the practical barriers that frequently impede researchers and educators from entering the field of ankle exoskeleton research. To meet this objective, the design follows three core principles: (i) all custom structural components must be manufacturable using consumer-grade desktop FDM 3D printers, (ii) all non-printed components must be standard off-the-shelf parts that are easily available, and (iii) the device must interface with commercially available footwear without permanent modification. Beyond these constraints, the design balances mechanical rigidity for effective torque transmission with a compact form factor suitable for experimental use. Furthermore, the system architecture is organized into clearly separated subsystems to facilitate rapid prototyping and the iteration of various assistance strategies. An overview of the hardware and major subsystems is shown in Fig. 1.

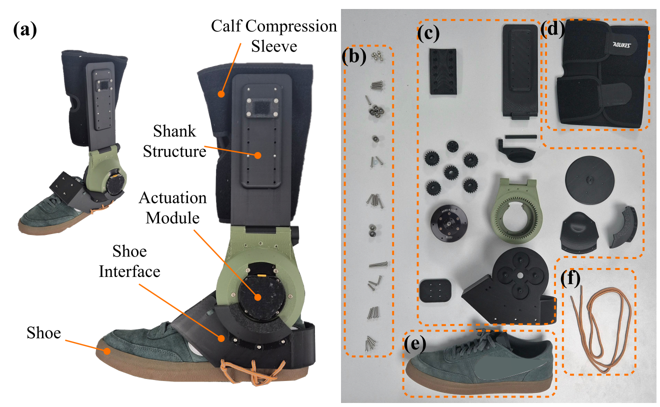

Fig. 1. **Overview of the PrintExo hardware.** (a) Fully assembled device. (b) Fasteners and bearings. (c) 3D-printed components and actuator. (d) Calf compression sleeve. (e) Example lace-up shoe. (f) Auxiliary lace.

B. Actuation and Structural Design

For the actuation module, a CubeMars AK60-6 V1.1 KV140 actuator (CubeMars, China) was selected for its commercial availability, lightweight profile (368 g), and built-in motor driver. The built-in driver simplifies the control architecture by streamlining communication and power management, making the system more accessible to researchers who may lack specialized electronics expertise. While this motor provides a peak torque of 9 N·m, prior ankle-exoskeleton studies have implemented peak assistive torques typically in the range of 10-30 N·m [34]–[36]. To meet this requirement, we designed an integrated 1:4 planetary gear stage with bearings integrated at each planet gear to minimize frictional losses and improve mechanical efficiency (Fig. 2). The motor, 3D-printed planetary stage, and protective casing form a compact actuation unit for efficient torque transmission.

The shank structure extends vertically from the actuation module and is positioned on the lateral side of the user's shank. Assistive torque is applied in the sagittal plane (plantarflexion/dorsiflexion), while a passive hinge accommodates frontal-plane inversion and eversion. This additional degree of freedom improves alignment with the user's natural gait kinematics and mitigates off-axis loads that could otherwise lead to mechanical damage. For secure attachment without custom-molded orthotics, the shank is secured using an off-the-shelf calf compression sleeve, providing a long contact length that resists rotation and slippage while distributing pressure evenly using readily available components.

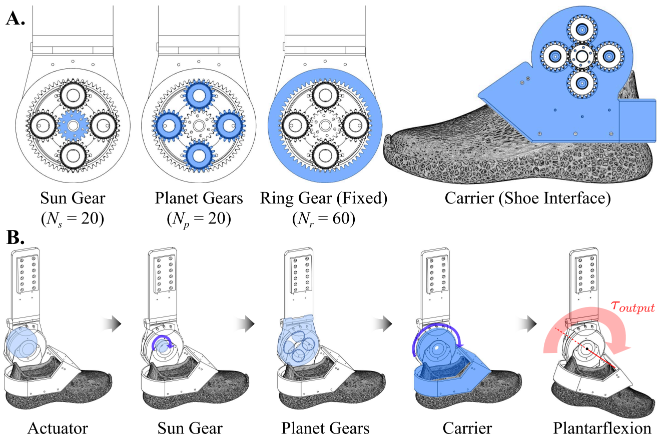

Fig. 2. **3D-printed planetary gearbox.** (A) Components of the planetary gearbox used in PrintExo, consisting of the sun gear ($N_s = 20$), four planet gears ($N_p = 20$), and a fixed ring gear ($N_r = 60$). The carrier is rigidly coupled to the shoe interface and serves as the torque output stage. (B) Schematic illustration of power transmission, where actuator drives the sun gear, transmitting torque through the planet gears to the carrier and producing an assistive plantarflexion torque about the anatomical ankle joint.

C. Shoe Interface Design

The lace-anchored shoe interface enables robust mechanical anchoring without permanent modification to the footwear. The interface includes a rigid dorsal component contoured to the midfoot, which extends diagonally toward the lateral side to connect with the planetary gear output of the actuation module. During fitting, the interface is positioned beneath the shoe laces and secured by routing the laces through integrated guides on the dorsal component, allowing it to be clamped between the tongue and the tensioned laces. To further resist rotation and slippage during dynamic movement, auxiliary laces are routed through guide holes in the plantar section of the interface and tightened across the sole of the shoe.

The interface provides a stiff load path for torque transfer during walking. During plantarflexion assistance, the dorsal structure bears against the shoe over the midfoot to transmit torque with minimal slip, while during swing and dorsiflexion, lace tension keeps the interface seated as the exoskeleton returns toward neutral without restricting natural ankle range of motion. To support diverse users and footwear, we release open-source files in multiple predefined size variants matched to standard shoe sizes, enabling rapid fitting across a wide range of commercial lace-up shoes without permanent modification.

IV. Fabrication & Implementation

PrintExo uses polylactic acid (PLA) filament for its custom components because of its high availability and ease of printing, which aligns with our objective of minimizing entry barriers. Previous studies have demonstrated the feasibility of PLA-based additive manufacturing in related load-bearing applications, including a 3D-printed prosthetic foot satisfying ISO 10328 static-strength requirements and a PLA+-based humanoid lower-body platform evaluated through structural analysis [37], [38]. Although PLA was used in this study to demonstrate viability with standard materials, the PrintExo design is also compatible with alternative filaments such as PETG or carbon-fiber-reinforced filaments.

All parts were printed on a Bambu Lab X1C (Bambu Lab, China) using a 0.4 mm nozzle, 0.20 mm layer height, and 70% gyroid infill pattern. To account for the anisotropic strength of layer-by-layer fabrication, key load-bearing components were oriented to avoid inter-layer shear as the dominant failure mode. To support reproducibility and broader use, all source files, including editable CAD (.f3d), neutral CAD (.step, .stp), mesh (.stl, .obj), and print-ready (.gcode) files, are publicly available through an open-access repository.

To improve parts availability and mechanical reliability, PrintExo uses standardized, off-the-shelf hardware for all load-bearing interfaces. Assembly requires only basic post-processing and simple tapping/drilling of pre-modeled holes, with fasteners standardized to M3 bolts and a single roller bearing size used throughout. The device can be assembled using common hand tools (optionally a power drill), and an open-source manual is provided with guidance for minor file edits to match locally available parts. The total assembled mass is 1.33 kg per leg, excluding the user's shoe. A complete bill of materials with sourcing links is provided in the open-source repository.

V. Feasibility Pilot Study

A. Methods

A feasibility pilot study was conducted with five able-bodied participants to evaluate the durability and feasibility of PrintExo. All participants provided informed consent, and the protocol was approved by the Korea University Institutional Review Board (KUIRB-2025-0516-01). Prior exoskeleton experience ranged from minimal to moderate.

Experiments were conducted on a treadmill at 1.0 m/s under three conditions in a fixed order: no-device (personal shoes only), zero-torque (PrintExo worn; motor enabled with $\tau = 0$), and powered-assistance (PrintExo worn with stride-by-stride active assistance) (Fig. 3). Each condition was 8 minutes with rest between conditions; in one participant, the powered-assistance trial was extended to 16 minutes to evaluate continuous-use feasibility. Outcome metrics were computed from a five-minute analysis window after metabolic measures stabilized.

During powered assistance, ankle torque was applied as a function of gait phase using a parameterized profile with a fixed peak magnitude of 15 N·m and fixed rise/fall time of 20%/10% of the gait cycle [7]. The peak timing was initialized per participant to a preferred timing selected at the beginning of the session and then held fixed during the powered trial. Gait phase was estimated in real time using the angular velocity measured by an inertial measurement unit (IMU) mounted on the dorsum of the shoe, enabling stride-synchronized application of the torque profile [39].

Gross metabolic power during walking was measured in all conditions using a wearable breath-analysis system (Neumafit PACER; Neumafit, South Korea). Lower-limb kinematics were recorded via optical motion capture (Vicon; Oxford Metrics, UK) during the no-device condition to compute biological ankle joint angles using the Plug-in Gait Lower Body model (Vicon Nexus). In the exoskeleton conditions (zero-torque and powered-assistance), the device ankle angle was obtained from the motor encoder. During powered assistance, motor-board temperature was additionally logged to assess thermal behavior during continuous operation.

The primary outcomes were durability and operational feasibility, assessed by trial completion without failure and stable interfaces enabling sequential reuse across participants. Secondary outcomes included gross metabolic power (W/kg), cycle-averaged angle behavior (biological angles from motion capture in the no-device condition and encoder-derived angles in exoskeleton conditions), and motor-board temperature during powered operation. Given the pilot nature of the study, results are reported descriptively to characterize feasibility and observed trends rather than to support population-level statistical claims.

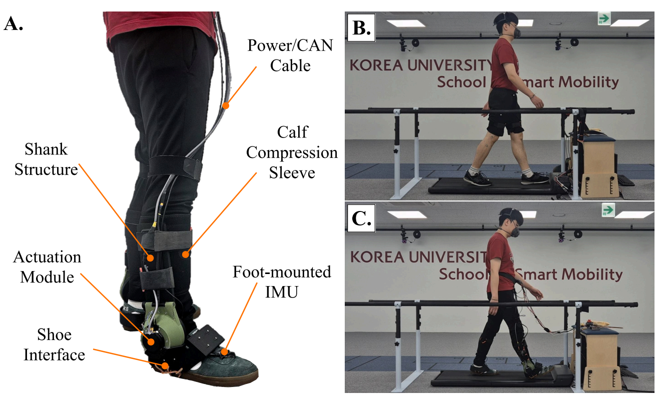

Fig. 3. **Experimental setup and device integration.** (A) PrintExo worn on the right leg, highlighting major structural components, interfaces, onboard sensing, and tethered cables for power and communication. (B) Treadmill walking under the no-device condition during optical motion capture (reflective markers attached). (C) Treadmill walking with PrintExo under zero-torque and powered-assistance conditions.

B. Results

PrintExo completed the full protocol without mechanical failure in four of five participants. Across these successful sessions, the device could be worn, operated, and reused sequentially between participants without requiring structural rework, supporting short-term operational feasibility of the 3D-printed hardware and interfaces under repeated treadmill use.

In one participant, the printed hinge fractured during powered assistance. After replacement, the repeated trial proceeded without hinge failure but was terminated due to substantial shank-interface twisting and slippage. An out-toed gait pattern was observed in this participant, which may have increased off-axis loading and contributed to the hinge and interface issues.

Across the four participants who completed all conditions successfully, gross metabolic power was consistently lowest in the no-device condition and increased when wearing the device. Under powered assistance, measured gross metabolic power was 4.24 ± 0.75 W/kg (mean ± standard deviation), compared with 4.41 ± 0.80 W/kg under zero-torque, corresponding to an observed mean reduction of 0.17 W/kg ($\sim$3.8%). Individual participant values across conditions are provided in Fig. 4.

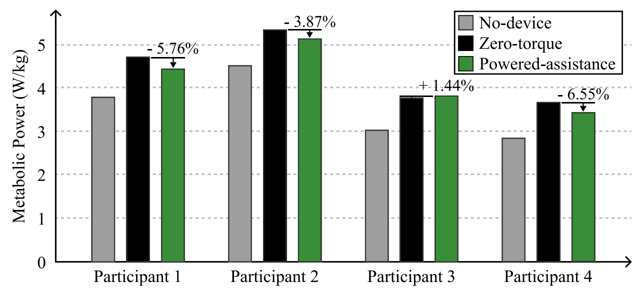

Fig. 4. **Participant-wise metabolic power across walking conditions.** Mass-normalized metabolic power (W/kg) is shown for the four participants who completed treadmill walking at 1.0 m/s under three conditions: no-device (personal shoes), zero-torque (PrintExo worn with motor enabled and $\tau = 0$), and powered-assistance (PrintExo with stride-synchronized plantarflexion assistance). Bars indicate each participant's mean metabolic power computed over the steady-state 5 min of each trial. Percentage annotations show the change in powered-assistance relative to zero-torque for each participant.

In the zero-torque condition, the exoskeleton encoder angle showed a gait-cycle progression similar to the no-device angle trajectory, suggesting that the exoskeleton hardware did not appear to restrict ankle motion. In contrast, during powered assistance, the encoder-derived device angle deviated earlier around the onset of the assistive torque profile and reached nearly 60° of plantarflexion. This reflects device-side motion rather than biological ankle joint motion (Fig. 5(B)). The torque command and the resulting cycle-averaged angle trajectory for a representative participant are shown in Fig. 5.

During powered operation, motor-board temperature increased over the 8-minute trials and reached a mean peak of 43.3 ± 2.5°C across participants who completed the standard protocol (n = 3; range: 39 - 46°C). In the extended 16-minute powered-assistance trial conducted in one participant, motor-board temperature continued to rise and reached 50°C by the end of the trial, indicating ongoing heat accumulation during prolonged continuous operation. No visible thermal deformation or material degradation of the 3D-printed components was observed in either the standard or extended trials.

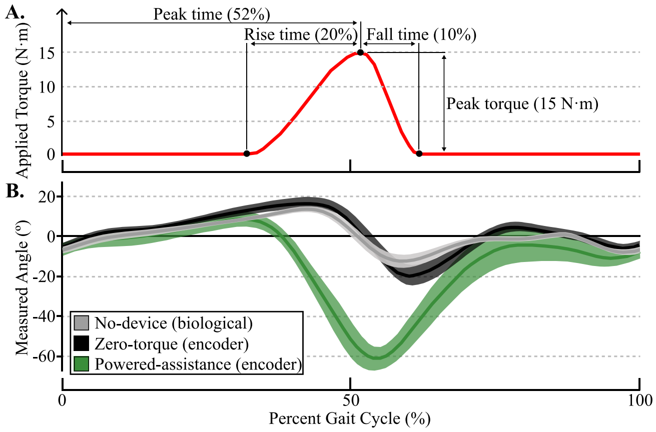

Fig. 5. **Assistive torque command and cycle-averaged angle trajectories over the gait cycle for a representative participant (participant 1).** (A) Stride-synchronized plantarflexion torque command parameterized by peak magnitude, peak timing, and rise/fall time. (B) Cycle-averaged angle trajectories for no-device (biological angle from motion capture), zero-torque (encoder), and powered-assistance (encoder); shaded regions indicate ±1 SD across strides. The large plantarflexion excursion under powered assistance represents device-side encoder motion rather than biological ankle joint motion. Dorsiflexion is positive.

VI. Discussion

The feasibility pilot study results suggest that a fully 3D-printable, open-source ankle exoskeleton can serve as a viable experimental platform for short-duration human walking studies. Across the completed sessions, PrintExo supported repeated treadmill use and sequential reuse without requiring structural rework. Together, these observations support the validity of the design goals: enabling rapid, independent replication and iteration of wearable-robotics protocols with human participants while keeping fabrication and setup overhead low. Accordingly, PrintExo is best positioned as a practical testbed for early-stage locomotion studies, where protocol flexibility and accessibility are intentionally prioritized over maximizing energetic benefit or torque-delivery efficiency.

PrintExo uses a lace-anchored, shoe-agnostic interface that attaches to commercially available lace-up shoes without permanent modification, enabling rapid fitting and sequential reuse across participants. This differs from many existing ankle exoskeletons, which rely on shoe-specific interfaces requiring permanent footwear modification or in-shoe contact components to achieve rigid torque transmission [2], [24], [32], [33]. While mechanically effective, such approaches increase setup overhead and typically constrain scalability to larger and more diverse participant cohorts, as compatible footwear and individualized fitting must be ensured. Our pilot results suggest that the lace-anchored interface provides sufficiently stable anchoring for short-duration treadmill walking, supporting early-stage studies where accessibility and ease of fitting and reuse are prioritized. However, gross metabolic power remained higher than in the no-device condition, suggesting that powered assistance did not fully offset the cost of wearing the 1.33 kg device. In addition, compliance at the shoe and calf-sleeve interfaces may produce relative motion between the device and biological ankle, reducing effective torque transmission during powered assistance. This trade-off reflects an intentional prioritization of accessibility over maximal mechanical efficiency and motivates future work to quantify delivered ankle torque and interface-level relative motion.

Under powered assistance, the observed actuator lead in encoder-derived ankle angles suggests that torque transmission is mediated by compliance at the human-robot interface rather than rigid joint coupling. Similar torque-driven behavior, in which motor actuation precedes biological joint motion, has been reported in prior ankle exoskeleton studies and attributed to interface compliance and relative motion [40]. Related experimental analyses further show that interface geometry and fixation strongly influence joint misalignment and interaction forces, indicating that soft tissue deformation, shoe compliance, and attachment configuration mediate this transient mismatch [41]. In the present system, the brief actuator lead implied by the encoder trends is likely absorbed by compliant elements such as soft tissue, the calf sleeve, and the shoe, consistent with the intentionally non-rigid anchoring strategy. This interpretation highlights a trade-off between accessibility and torque transmission fidelity and motivates future work to quantify delivered ankle torque, interface-level relative motion, and their implications for user comfort and safety.

Several limitations of this pilot study should be acknowledged. First, the validation involved a small number of able-bodied participants and used a fixed condition order to prioritize safe familiarization, which limits generalizability and may introduce adaptation or fatigue effects. Second, methodological constraints limited biomechanical interpretation. Gross metabolic power was measured using a wearable system rather than a laboratory cart, and the observed difference should be further validated against measurement variability before being interpreted as an energetic benefit. Biological ankle kinematics were available only in the no-device condition because the required motion-capture marker locations overlapped with the exoskeleton hardware. The protocol also used a single fixed speed and did not measure propulsion-related outcomes (e.g., ground reaction forces), limiting inference beyond metabolic trends. Future studies should use an exoskeleton-compatible marker set with model-based kinematic analysis to quantify biological ankle motion during powered assistance. Third, the assistance profile was not systematically optimized for individual participants and may therefore have been insufficient to offset the added device mass and interface-related transmission losses. Fourth, one participant experienced hinge fracture and subsequent shank-interface instability, suggesting sensitivity to off-axis loading and non-neutral gait patterns such as out-toeing. Finally, longer-duration operation was not systematically evaluated, and the fatigue life and thermal margins of the 3D-printed components remain incompletely characterized. The observed hinge fracture suggests that localized stress concentration and off-axis loading may represent critical failure modes under repeated high-torque operation.

Building on the pilot findings, future work will strengthen

PrintExo as a robust, extensible experimental platform by reinforcing high-stress components such as the hinge, improving off-axis tolerance, and quantifying fatigue life and thermal durability through endurance testing and simulation. Expanded validation with larger cohorts and exoskeleton-compatible measurements will better characterize biomechanical and energetic outcomes [3]. We will also evaluate wearable IMU-based kinematic estimation [42], [43] and integrate additional sensing (e.g., pressure insoles and other wearable/vision modalities) to estimate propulsion, ground reaction forces, and environmental context for more adaptive control [44]–[46]. In parallel, we will maintain a versioned open-source release with iterative updates to hardware variants, documentation, and educational examples to support reproducible use across labs and classrooms.

VII. CONCLUSIONS

This work presented PrintExo, an open-source, shoe-agnostic, and 3D-printable ankle exoskeleton platform for accessible locomotion research and rapid prototyping. By combining consumer-grade FDM manufacturing with a lace-anchored shoe interface, the system enables fabrication and fitting without permanent footwear modification or specialized infrastructure. Pilot treadmill validation demonstrated short-duration operational feasibility and revealed device-side kinematic characteristics relevant to torque transmission. While further work is needed to improve durability, quantify delivered ankle torque, and expand experimental rigor, PrintExo provides a practical baseline that can evolve through open, community-driven development.

APPENDIX

All CAD files, BOM, and assembly documentation are available at `https://printexo.github.io`.

ACKNOWLEDGMENT

This research was supported by a grant of the Korean ARPA-H Project through the Korea Health Industry Development Institute (KHIDI), funded by the Ministry of Health & Welfare, Republic of Korea (grant number : RS-2025-25455839).

REFERENCES

[1] G. S. Sawicki *et al.*, “The exoskeleton expansion: improving walking and running economy,” *Journal of NeuroEngineering and Rehabilitation*, vol. 17, no. 1, p. 25, 2020.

[2] P. Slade *et al.*, “Personalizing exoskeleton assistance while walking in the real world,” *Nature*, vol. 610, no. 7931, pp. 277–282, 2022.

[3] R. W. Nuckols *et al.*, “Design and evaluation of an independent 4-week, exosuit-assisted, post-stroke community walking program,” *Annals of the New York Academy of Sciences*, vol. 1525, no. 1, pp. 147–159, 2023.

[4] J. Kim *et al.*, “Soft robotic apparel to avert freezing of gait in Parkinson’s disease,” *Nature Medicine*, vol. 30, no. 1, pp. 177–185, 2024.

[5] J. Moon *et al.*, “Reducing sprint time with exosuit assistance in the real world,” *Science Robotics*, vol. 8, no. 82, Art. no. eadf5611, 2023.

[6] G. Lee *et al.*, “Reducing the metabolic cost of running with a tethered soft exosuit,” *Science Robotics*, vol. 2, no. 6, Art. no. eaan6708, 2017.

[7] J. Zhang *et al.*, “Human-in-the-loop optimization of exoskeleton assistance during walking,” *Science*, vol. 356, no. 6344, pp. 1280–1284, 2017.

[8] R. R. Neptune *et al.*, “Contributions of the individual ankle plantar flexors to support, forward progression and swing initiation during walking,” *Journal of Biomechanics*, vol. 34, no. 11, pp. 1387–1398, 2001.

[9] A. Kian *et al.*, “Application of wearable sensors in actuation and control of powered ankle exoskeletons: A comprehensive review,” *Sensors*, vol. 22, no. 6, Art. no. 2244, 2022.

[10] J. R. Williams *et al.*, “OpenExo: An open-source modular exoskeleton to augment human function,” *Science Robotics*, vol. 10, no. 103, Art. no. eadt1591, 2025.

[11] W. Meng *et al.*, “Soft ankle-foot exoskeleton for rehabilitation: A systematic review of actuation, sensing, mechanical design, and control strategy,” *IEEE Transactions on Medical Robotics and Bionics*, vol. 6, no. 2, pp. 384–398, 2024.

[12] D. Hanson *et al.*, “Open Arms: Open-Source Arms, Hands & Control,” *arXiv preprint* arXiv:2205.12992, 2022.

[13] S. Mick *et al.*, “Reachy, a 3D-printed human-like robotic arm as a testbed for human-robot control strategies,” *Frontiers in Neurorobotics*, vol. 13, Art. no. 65, 2019.

[14] J. Glossner *et al.*, “An overview of the drone open-source ecosystem,” *arXiv preprint* arXiv:2110.02260, 2021.

[15] F. Arvin *et al.*, “Mona: an affordable open-source mobile robot for education and research,” *Journal of Intelligent & Robotic Systems*, vol. 94, no. 3, pp. 761–775, 2019.

[16] S. N. Yousaf *et al.*, “A Method for the Analysis of Physical Human-Robot Interaction,” in *Proc. IEEE/ASME Int. Conf. Advanced Intelligent Mechatronics (AIM)*, 2021, pp. 1249–1254.

[17] A. B. Zoss *et al.*, “Biomechanical Design of the Berkeley Lower Extremity Exoskeleton (BLEEX),” *IEEE/ASME Transactions on Mechatronics*, vol. 11, no. 2, pp. 128–138, 2006.

[18] M. B. Näf *et al.*, “Misalignment Compensation for Full Human-Exoskeleton Kinematic Compatibility: State of the Art and Evaluation,” *Applied Mechanics Reviews*, vol. 70, no. 5, Art. no. 050802, 2018.

[19] M. Cenciarini *et al.*, “Biomechanical considerations in the design of lower limb exoskeletons,” in *Proc. IEEE Int. Conf. Rehabilitation Robotics (ICORR)*, 2011, Art. no. 5975366.

[20] G. Pelin *et al.*, “The use of additive manufacturing techniques in the development of polymeric molds: a review,” *Polymers*, vol. 16, no. 8, Art. no. 1055, 2024.

[21] M. Dezman *et al.*, “Ankle Exoskeleton with a Symmetric 3 DoF Structure for Plantarflexion Assistance,” in *Proc. IEEE Int. Conf. Robotics and Automation (ICRA)*, 2024, pp. 3227–3233.

[22] G. Orekhov *et al.*, “Usability and performance validation of an ultra-lightweight and versatile untethered robotic ankle exoskeleton,” *Journal of NeuroEngineering and Rehabilitation*, vol. 18, Art. no. 163, 2021.

[23] Z. Wang *et al.*, “A Cost-Effective Lightweight Hip Exoskeleton for Material Handling,” in *Proc. IEEE/ASME Int. Conf. Advanced Intelligent Mechatronics (AIM)*, 2025.

[24] Z. F. Lerner *et al.*, “An untethered ankle exoskeleton improves walking economy in a pilot study of individuals with cerebral palsy,” *IEEE Transactions on Neural Systems and Rehabilitation Engineering*, vol. 26, no. 10, pp. 1985–1993, 2018.

[25] G. M. Bryan *et al.*, “A hip–knee–ankle exoskeleton emulator for studying gait assistance,” *International Journal of Robotics Research*, vol. 40, no. 4–5, pp. 722–746, 2021.

[26] B. W. K. Ang *et al.*, “Print-it-Yourself (PIY) glove: A fully 3D printed soft robotic hand rehabilitative and assistive exoskeleton for stroke patients,” in *Proc. IEEE/RSJ Int. Conf. Intelligent Robots and Systems (IROS)*, 2017.

[27] D. Esposito *et al.*, “Design of a 3D-printed hand exoskeleton based on force-myography control for assistance and rehabilitation,” *Machines*, vol. 10, no. 1, Art. no. 57, 2022.

[28] M. Muehlhaus *et al.*, “ExoKit: A Toolkit for Rapid Prototyping of Interactions for Arm-based Exoskeletons,” in *Proc. CHI Conf. Human Factors in Computing Systems*, 2025.

[29] E. Urendes *et al.*, “Design, development, and functional validation of a 3D-printed passive upper limb exoskeleton,” *IEEE Transactions on Neural Systems and Rehabilitation Engineering*, 2024.

[30] V. V. Patel *et al.*, “Open robot hardware: progress, benefits, challenges, and best practices,” *IEEE Robotics & Automation Magazine*, vol. 30, no. 3, pp. 123–148, 2022.

[31] K. A. Ingraham *et al.*, “The role of user preference in the customized

control of robotic exoskeletons," *Science Robotics*, vol. 7, no. 64, Art. no. eabj3487, 2022.

[32] O. N. Beck *et al.*, "Exoskeletons need to react faster than physiological responses to improve standing balance," *Science Robotics*, vol. 8, no. 75, Art. no. eadf1080, 2023.

[33] N. Van Crey *et al.*, "Design of a quasi-passive ankle-foot orthosis with customizable, variable stiffness," in *Proc. Int. Conf. Rehabilitation Robotics (ICORR)*, 2023.

[34] G. Orekhov *et al.*, "Design and electromechanical performance evaluation of a powered parallel-elastic ankle exoskeleton," *IEEE Robotics and Automation Letters*, vol. 7, no. 3, pp. 8092–8099, 2022.

[35] B. Chen *et al.*, "Development and Validation of Robotic Ankle Exoskeleton With Parallel Nonlinear Elastic Actuator," *Journal of Mechanical Design*, vol. 146, no. 11, Art. no. 113304, 2024.

[36] R. L. Medrano *et al.*, "Can humans perceive the metabolic benefit provided by augmentative exoskeletons?," *Journal of NeuroEngineering and Rehabilitation*, vol. 19, no. 1, p. 26, 2022.

[37] A. M. Gómez-Amador *et al.*, "3D-printed prosthetic foot design: Mechanical similarity and testing," *Materials & Design*, vol. 253, art. no. 113918, 2025.

[38] A. J. Fuge *et al.*, "Design, development, and analysis of the lower body of next-generation 3D-printed humanoid research platform: PANDORA," *Robotica*, vol. 41, no. 7, pp. 2177–2206, 2023.

[39] I. P. I. Pappas *et al.*, "A reliable gyroscope-based gait-phase detection sensor embedded in a shoe insole," *IEEE Sensors Journal*, vol. 4, no. 2, pp. 268–274, 2004.

[40] J. F. Almeida, J. C. André, and C. P. Santos, "Ankle exoskeletons in walking and load-carrying tasks: Insights into biomechanics and human-robot interaction," *IRBM*, 2025, Art. no. 100911.

[41] R. L. Andrade *et al.*, "Human-robot joint misalignment, physical interaction, and gait kinematic assessment in ankle-foot orthoses," *Sensors*, vol. 24, no. 1, Art. no. 246, 2023.

[42] D. Kim *et al.*, "Learning-based 3D human kinematics estimation using behavioral constraints from activity classification," *Nature Communications*, vol. 16, no. 1, Art. no. 3454, 2025.

[43] B. Hur *et al.*, "Learning based lower limb joint kinematic estimation using open source IMU data," *Scientific Reports*, vol. 15, no. 1, Art. no. 5287, 2025.

[44] K. Swaminathan *et al.*, "Multi-modal sensing for propulsion estimation in people post-stroke across speeds," *IEEE Transactions on Neural Systems and Rehabilitation Engineering*, 2025.

[45] G. Bergamo *et al.*, "Individualized learning-based ground reaction force estimation in people post-stroke using pressure insoles," in *Proc. IEEE Int. Conf. Rehabil. Robot. (ICORR)*, 2023.

[46] L. Gionfrida *et al.*, "Wearable robots for the real world need vision," *Science Robotics*, vol. 9, no. 90, Art. no. eadj8812, 2024.